

Inferential Iterative Learning Control: A 2D-System Approach

Joost Bolder^a and Tom Oomen^a

^a*Eindhoven University of Technology, Dept. of Mechanical Engineering, Control Systems Technology group, P.O. Box 513, 5600 MB Eindhoven, The Netherlands*

Abstract

Certain control applications require that performance variables are explicitly distinguished from measured variables. The performance variables are not available for real-time feedback. Instead, they are often available after a task. This enables the application of batch-to-batch control strategies such as Iterative Learning Control (ILC) to the performance variables. The aim of this paper is first to show that the pre-existing ILC controllers may not be directly implementable in this setting, and second to develop a new approach that enables the use of different variables for feedback and batch-to-batch control. The analysis reveals that by using pre-existing ILC methods, the ILC and feedback controllers may not be stable in an inferential setting. Therefore, the complete closed-loop system is cast in a 2D framework to analyze stability. Several solution strategies are outlined. The analysis is illustrated through an application example in a printing system. Finally, the developed theory also leads to new results for traditional ILC algorithms in the common situation where the feedback controller contains a pure integrator.

Key words: Iterative learning control, inferential control, 2D system, stability along the pass, limit profile

1 Introduction

Increasing performance requirements on systems demand an explicit distinction between measured variables and performance variables. Performance variables may not be available for real-time feedback control due to computational constraints, physical limitations in sensor placement, delays in acquiring measurements, etc. Examples include heat exchangers [1] and motion systems [2].

In many cases, the performance variables are available off-line. For instance, when the final product is inspected afterwards, the ‘true’ performance is revealed. This enables batch-to-batch control using performance variables. A common batch-to-batch control strategy is Iterative Learning Control (ILC) [3]. In ILC, the control signal is updated trial-to-trial using measurement data of previous trials to improve performance. Traditionally, ILC is applied to the measured variables that are also available for the feedback controller. This classical approach is well-established with many results on the convergence and robustness properties [4,5].

A direct combination of ILC acting on the performance variables while the feedback controller uses different real-time measured variables may lead to potentially hazardous situations. Indeed, the feedback controller aims to regulate the

measured variables while the ILC regulates the performance variables. This may lead to a conflict in case a parallel [3] ILC-feedback control structure is used. In [6], initial indications of such a conflict are already reported. In [7], a related and specific approach is presented to use observers to *infer* the performance variables from the real-time measurements instead of a direct performance measurement. The main idea is that distinguishing between performance and measured variables can potentially fully exploit the use of ILC. The use of performance variables for ILC and different real-time measured variables for feedback control is referred to as *inferential ILC* in the present paper.

Although ILC is potentially promising for the mentioned inferential control applications, the direct application of pre-existing ILC design methods may not lead to satisfactory performance and stability properties. In fact, in this paper it is shown through a formal analysis that using traditional ILC design approaches such as [3,4] in the inferential ILC situation can lead to implementations that are unstable.

The main result of this paper is a framework for inferential ILC, including a detailed analysis and new learning control approaches. To facilitate the analysis, the time-trial dynamics of a common ILC algorithm with dynamic learning filters is cast into a 2D Framework using discrete Linear Repetitive Processes (dLRP’s) [8]. The motivation for using 2D systems stems from the observation that the unstable behavior remains undetected in traditional approaches, e.g., as the

Email addresses: jbolder@gmail.com (Joost Bolder),
t.a.e.oomen@tue.nl (Tom Oomen).

lifted/supervector approach in [4]. Stability conditions are developed using 2D systems theory. Solutions are presented and analyzed using these stability conditions. The analysis is illustrated through an application example in printing systems. In addition, it can be shown that the related approach in [7] can be analyzed in the developed framework as a special case. Finally, the developed theory also leads to new results for the traditional ILC case where the performance variables are equal to the measured variables in the common situation where the feedback controller contains an integrator.

Notation \mathbb{Z}^* (\mathbb{Z}^+) denotes the set of positive (non-negative) integers. Discrete-time is denoted with $p \in \mathbb{Z}$, $k \in \mathbb{Z}$ is the trial index. For $A \in \mathbb{C}^{n \times n}$, $\rho(A) = \max_{1 \leq i \leq n} |\lambda_i|$, with $\lambda = \{\lambda_0, \lambda_1, \dots, \lambda_n\}$ the spectrum of A . Systems are discrete-time, for a system G , $G := \begin{bmatrix} A^G & B^G \\ C^G & D^G \end{bmatrix}$ denotes a state-space representation with state x^G , which is often assumed minimal. The real-rational transfer function for G is given by $G(z) = C^G(zI - A^G)^{-1} + D^G$, with z a complex indeterminate and $G \in \mathcal{R}^{n_y \times n_u}$. Over a finite-time interval $0 \leq p < \alpha$, $\alpha \in \mathbb{Z}^+$, the input-output behavior of G can be denoted as $\bar{y} = \bar{G}\bar{u}$ with $\bar{G} \in \mathbb{R}^{\alpha n_y \times \alpha n_u}$ a Toeplitz matrix that contains the impulse response coefficients $h(p)$, where $h(p) = C^G(A^G)^{p-1}B^G$ for $p > 0$ and $h(0) = D^G$, with $h(p) \in \mathbb{R}^{n_y \times n_u}$ [4]. The input $\bar{u} \in \mathbb{R}^{\alpha n_u}$ and output $\bar{y} \in \mathbb{R}^{\alpha n_y}$. Single-input single-output systems are assumed throughout to facilitate the presentation. The extension to multivariable systems is conceptually straightforward and many of the results in Section 3 and Section 4 directly apply.

2 Problem definition and application motivation

First, the control setup is motivated from an application perspective. Next, the considered problem is presented.

2.1 Application motivation and control setup

Printing systems are an important example where performance variables cannot be measured directly in real-time. The paper positioning drive of a printer, see Fig. 1, is traditionally controlled through feedback using inexpensive encoder position measurements. High tracking accuracy using the encoder measurement y does not imply good printing performance z due to mechanical deformations in the drive.

Recently, a scanner has been mounted in the printhead, which enables line-by-line measurements of the printing performance z [9]. This direct measurement of the performance is not available to real-time feedback, but can directly be used for batch-to-batch control strategies including Iterative Learning Control (ILC). This leads to the situation where the variables for feedback control y are not equal to variables for ILC z , see Fig. 2. Here, $\begin{bmatrix} z_k & y_k \end{bmatrix}^T = Pu_k$. System P has two outputs: the performance variable z_k and the measured variable y_k . The input to the system equals $u_k = u_k^C + f_k$.

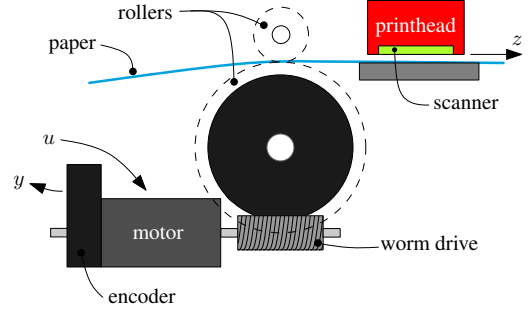


Fig. 1. Side-view of the positioning drive in a printer. The paper position z is controlled using the motor. The feedback controller uses real-time encoder measurements y . The performance z is measured line-by-line using the scanner.

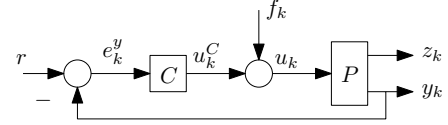


Fig. 2. Traditional feedback control setup.

Here, $u_k^C(r, y_k)$ is the feedback control signal. In traditional printing systems, it is assumed that $y_k \approx z_k$, in which case a feedback controller is implemented as $u_k^C = C(r - y_k)$, with C assumed fixed and designed such that the closed-loop system is internally stable. In the setting considered in the present paper, the feedforward signal f_k results from a batch-to-batch control algorithm. For instance, standard ILC approaches [3] consider an algorithm of the form

$$f_{k+1} = Q(f_k + Le_k^z), \quad (1)$$

where $e_k^z = r - z_k$, L is a learning filter, Q is a robustness filter, and k is the trial index. Appropriate substitution of e_k^z in (1) using $P = \begin{bmatrix} P^z & P^y \end{bmatrix}^T$, $z_k = P^z u_k$, $u_k = Ce_k^y + f_k$, $e_k^y = r - y_k$, and $y_k = P^y u_k$ leads to iteration domain dynamics $f_{k+1} = Q(1 - LJ)f_k + L(1 - JC)r$, where

$$J = \frac{P^z}{1 + CP^y}. \quad (2)$$

Next, a simplified inferential ILC example is presented.

2.2 Illustrative example

In the following example, it is shown that using the traditional ILC approach of [3] in the batch-to-batch inferential setting where $y_k \neq z_k$ can lead to an undesirable situation.

Example 1 Let $P = \begin{bmatrix} P^z \\ P^y \end{bmatrix} = \begin{bmatrix} 1 \\ 3 \end{bmatrix}$ and $C = \begin{bmatrix} 1 & 1 \\ 0.5 & 0 \end{bmatrix}$.

Thus, P is a static system and C an I-controller. The stable

closed-loop system is given by

$$\begin{bmatrix} z_k \\ y_k \end{bmatrix} = \begin{bmatrix} -0.5 & 1 & 3 \\ -0.5 & 0 & 1 \\ -1.5 & 0 & 3 \end{bmatrix} \begin{bmatrix} r \\ f_k \end{bmatrix}.$$

Next, an ILC algorithm (1) is designed following [4,3], with $Q = 1$ and L such that the trial-to-trial dynamics converge. The converged command signal f_∞ is given by

$$f_\infty = \lim_{k \rightarrow \infty} f_{k+1} = (1 + CP^y - CP^z)P^{z-1}r, \quad (3)$$

and the resulting limit error $e_\infty^z = 0$. Next, note that a minimal state-space realization for (3) and e_∞^z is given by

$$\begin{bmatrix} f_\infty \\ e_\infty^z \end{bmatrix} = \underbrace{\begin{bmatrix} 1 & -2 \\ -0.5 & 1 \\ 0 & 0 \end{bmatrix}}_F r. \quad (4)$$

In this case, a bounded nonzero r yields $e_\infty^z = 0$, however, f_∞ may be unbounded due to a pole $z = 1$ in $F(z)$.

This example reveals that a hazardous situation occurs in case $P^y \neq P^z$, although a typical ILC approach is followed, i.e., a stable closed loop system and a convergent ILC algorithm. The feedback controller aims to regulate e_k^y and the ILC regulates e_k^z . If $e_k^z = 0$ then $e_k^y \neq 0$ due to $P^z \neq P^y$ and a nonzero r . The integrator in C integrates e_k^y , yielding a unbounded growing signal. The ILC compensates this behavior by generating an opposite signal, see (3) and (4) that yields $e_k^z = 0$. The latter example is analyzed in more detail using the developed framework in Section 4 and Section 5.

A main consequence in practice includes unbounded system input signals after minimal changes in system dynamics or the feedback controller. Essentially, if any of the systems in the control loop are changed, or fail, the input to the system may be unbounded as well, with potentially disastrous consequences.

The assumption $Q = 1$ is to facilitate the presentation, the analysis and conclusions are also applicable to cases with Q -filtering.

2.3 Problem formulation and contributions

In this paper, inferential ILC is investigated: ILC using off-line measurements of the performance variables z while feedback uses real-time measurements y . The problem addressed in this paper is the formal stability analysis of this situation. This paper includes the following contributions, which are sequentially addressed in Section 2-6.

- (1) Illustration of stability problems in inferential ILC.

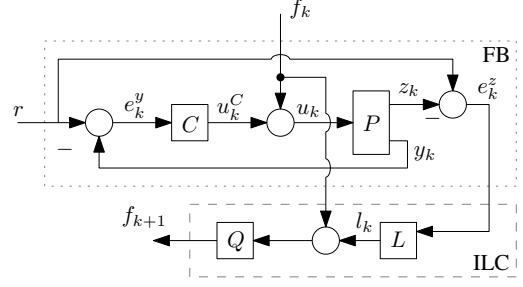


Fig. 3. Inferential control setup with traditional feedback control and the ILC algorithm implemented.

- (2) Analysis and solutions using a 2D-systems approach.
- (3) Presentation of new insights in the classical $y = z$ ILC case when C includes integral action.
- (4) The results are supported with numerical examples.

Preliminary research related to contributions 1 and 2 appeared in [10,11]. The present paper extends these initial findings with theory, explanations, examples, and contributions 3 and 4.

3 Linear repetitive process framework for inferential ILC

Example 1 revealed that standard ILC designs can lead to unbounded control signals in the inferential $y \neq z$ setting. Standard analyses using the lifted/supervector approach, see e.g. [4,3], do not reveal the aspect of unbounded control signals as shown in the example in Section 2.2. In this paper, an extended analysis with $y \neq z$ is performed by casting the ILC algorithm into a discrete linear repetitive process, see [8] and [12] for a definition.

State-space representations for the system P and feedback controller C are given by

$$P = \begin{bmatrix} A^P & B^P \\ C^{Pz} & D^{Pz} \\ C^{Py} & D^{Py} \end{bmatrix}, \quad \text{and} \quad C = \begin{bmatrix} A^C & B^C \\ C^C & 0 \end{bmatrix}. \quad (5)$$

The output state-space matrices for P are partitioned according to the dimensions of z_k and y_k . The strict properness of C guarantees well-posedness and facilitates the presentation. In addition, state-space representations for L and Q in (1) are given by

$$Q = \begin{bmatrix} A^Q & B^Q \\ C^Q & D^Q \end{bmatrix}, \quad \text{and} \quad L = \begin{bmatrix} A^L & B^L \\ C^L & D^L \end{bmatrix}. \quad (6)$$

Figure 3 shows the inferential ILC setup with traditional feedback control implemented. First consider the general form of a dLRP in Definition 2.

Definition 2 A discrete linear repetitive process is given by

$$\begin{aligned} \mathcal{X}_{k+1}(p+1) &= \mathcal{A}\mathcal{X}_{k+1}(p) + \mathcal{B}\mathcal{U}_{k+1}(p) + \mathcal{B}_0\mathcal{Y}_k(p), \\ \mathcal{Y}_{k+1}(p) &= \mathcal{C}\mathcal{X}_{k+1}(p) + \mathcal{D}\mathcal{U}_{k+1}(p) + \mathcal{D}_0\mathcal{Y}_k(p). \end{aligned} \quad (7)$$

Discrete-time is denoted by $p \in \mathbb{Z}$, with $0 \leq p < \alpha$, $\alpha \in \mathbb{Z}^+$. The pass index is denoted as $k \in \mathbb{Z}^*$. Here $\mathcal{X}_k(p)$ is the state, $\mathcal{Y}_k(p)$ is the pass-profile, and $\mathcal{U}_k(p)$ the input.

To cast the ILC structure in Fig. 3 into (7), let $\mathcal{X}_{k+1}(p) = \begin{bmatrix} x_{k+1}^P(p) & x_{k+1}^C(p) & x_{k+1}^L(p) & x_{k+1}^Q(p) \end{bmatrix}^T$, in accordance with (5) and (6), in addition, $\mathcal{Y}_k(p) = f_{k+1}(p)$. The input of the dLRP is the reference r , hence $\mathcal{U}_{k+1}(p) = r(p)$ which is pass-invariant. The boundary conditions $\mathcal{X}_{k+1}(0)$ and $\mathcal{Y}_0(p)$ are assumed constant throughout, which is a standard assumption in ILC [3]. The matrices $\mathcal{A}, \mathcal{B}, \mathcal{B}_0, \mathcal{C}, \mathcal{D}$, and \mathcal{D}_0 follow using (5), (6) and interconnection relations $e_k^z = r - z_k$ and $u_k = C(r - y_k) + f_k$, and are given by

$$\begin{aligned} \mathcal{A} &= \begin{bmatrix} A^P & B^P C^C & 0 & 0 \\ -B^C C^{P_y} & A^C - B^C D^{P_y} C^C & 0 & 0 \\ -B^L C^{P_z} & -B^L D^{P_z} C^C & A^L & 0 \\ -B^Q D^L C^{P_z} & -B^Q D^L D^{P_z} C^C & B^Q C^L & A^Q \end{bmatrix} \mathcal{B} = \begin{bmatrix} 0 \\ B^C \\ B^L \\ B^Q D^L \end{bmatrix} \mathcal{B}_0 = \begin{bmatrix} B^P \\ -B^C D^{P_y} \\ -B^L D^{P_z} \\ B^Q (I - D^L D^{P_z}) \end{bmatrix} \\ \mathcal{C} &= \begin{bmatrix} -D^Q D^L C^{P_z} & -D^Q D^L D^{P_z} C^C & D^Q C^L & C^Q \end{bmatrix} \mathcal{D} = \begin{bmatrix} D^Q D^L \end{bmatrix} \mathcal{D}_0 = \begin{bmatrix} D^Q (I - D^L D^{P_z}) \end{bmatrix}. \end{aligned} \quad (8)$$

In the next section, a formal 2D stability analysis of inferential ILC is presented using the dLRP in (7) and (8).

4 Stability aspects

The aim in this section is to investigate f_∞ in (3) and the stability aspects of (1) in the inferential setting. Relevant stability notions for dLRPs are connected with classical ILC convergence conditions. These connections form the basis for solutions and also expose how the unstable behavior remains undetected in traditional ILC design approaches.

4.1 Asymptotic stability and analysis of the limit profile

Asymptotic stability for dLRPs is a common definition of stability and is investigated first. Assume a pass-invariant input $\mathcal{U}_{k+1} = \mathcal{U}_\infty$ in (7) as is the case in the present ILC setting with $\mathcal{U}_\infty = r(p)$. Essentially, asymptotic stability guarantees that the pass profile \mathcal{Y}_k converges to a limit profile $\mathcal{Y}_\infty = \lim_{k \rightarrow \infty} \mathcal{Y}_k$ when a pass-invariant input \mathcal{U}_∞ is applied for a finite pass-length α . Consider the following lemma.

Lemma 3 (Asymptotic stability) The dLRP in (7) is asymptotically stable if and only if $\rho(\mathcal{D}_0) < 1$.

Proof See [8, Corollary 2.1.3] or [12, Theorem 3.3.4].

The condition in Lemma 3 is directly applicable to the ILC algorithm (1), leading to the following result.

Theorem 4 The dLRP in (7), with matrices (8) is asymptotically stable if and only if $\rho(\bar{Q}(I - \bar{L}\bar{J})) < 1$, with \bar{Q}, \bar{L} , and \bar{J} the Toeplitz matrix representations of Q, L , and J in (6) and (2).

Proof From (5) and (8) it follows that \mathcal{D}_0 is the direct feedthrough of $Q(1 - LJ)$. Next, $\bar{Q}(I - \bar{L}\bar{J})$ is lower-triangular with \mathcal{D}_0 on the diagonal since Q, L and J are causal. Hence, $\rho(\bar{Q}(I - \bar{L}\bar{J})) = \rho(\mathcal{D}_0)$ follows directly.

Theorem 4 shows that asymptotic stability for dLRPs is identical to the finite-time convergence condition $\rho(\bar{Q}(1 - \bar{L}\bar{J})) < 1$ developed in [4, Theorem 1].

The following results are essential to show that the resulting limit profile f_∞ may be unbounded, even though $\rho(\bar{Q}(1 - \bar{L}\bar{J})) < 1$ and C being an internally stabilizing controller.

Lemma 5 (Limit profile) Given an asymptotically stable dLRP, a pass-invariant input sequence $\mathcal{U}_{k+1} = \mathcal{U}_k = \mathcal{U}_\infty$, and boundary conditions $\mathcal{X}_{k+1}(0) = 0, \mathcal{Y}_0(p) = 0$. Then, the state-space system that generates the limit profile $\mathcal{Y}_\infty = \lim_{k \rightarrow \infty} \mathcal{Y}_k$ for the inferential ILC system (7) is given by

$$\mathcal{Y}_\infty = \begin{bmatrix} \mathcal{A}_\infty & \mathcal{B}_\infty \\ \mathcal{C}_\infty & \mathcal{D}_\infty \end{bmatrix} \mathcal{U}_\infty \quad (9)$$

$$\begin{aligned} \mathcal{A}_\infty &= [\mathcal{A} + \mathcal{B}_0(I - \mathcal{D}_0)^{-1}\mathcal{C}], \quad \mathcal{C}_\infty = (I - \mathcal{D}_0)^{-1}\mathcal{C} \\ \mathcal{B}_\infty &= [\mathcal{B} + \mathcal{B}_0(I - \mathcal{D}_0)^{-1}\mathcal{D}], \quad \mathcal{D}_\infty = (I - \mathcal{D}_0)^{-1}\mathcal{D} \end{aligned}$$

Proof Following the lines in [12, Section 3.1, pp. 112], [8, Section 2.1, pp. 50], and computing the steady-state value in pass-to-pass direction using $k = k + 1 := \infty$ in (7) and rearranging yields (9).

Theorem 6 Let $Q = 1$ and $\rho(\bar{Q}(I - \bar{L}\bar{J})) < 1$. Then, a state-space realization for f_∞ in (3) is given by

$$f_\infty = \left[\begin{array}{cc|c} A^P - B^P D^{P_z^{-1}} C^{P_z} & 0 & B^P D^{P_z^{-1}} \\ -B^C (C^{P_y} - D^{P_y} D^{P_z^{-1}} C^{P_z}) & A^C & B^C (I - D^{P_y} D^{P_z^{-1}}) \\ \hline -D^{P_z^{-1}} C^{P_z} & -C^C & D^{P_z^{-1}} \end{array} \right] r. \quad (10)$$

Proof The state-space representation for the limit profile f_∞ follows by substituting $D^Q = 1, A^Q = \emptyset, B^Q = \emptyset$ and $C^Q = \emptyset$ in (8), and the latter in (9) in Lemma 5.

Consider the system matrix of the state-space system that generates f_∞ in (10). It shows that this matrix has a lower-triangular structure, hence the eigenvalues of this matrix include the eigenvalues of A^C .

Example revisited - 1 In example 1 $\lambda_0(A^C) = 1$. Thus $\rho(\mathcal{A}_\infty) = 1$, resulting in an unstable limit system.

A stronger notion of stability is necessary to guarantee $\rho(\mathcal{A}_\infty) < 1$ in Lemma 5. Indeed, this is also recognized in

[8, Chapter 9, pp. 369] where ILC and feedback are jointly synthesized for the $y = z$ situation. Therefore, the notion of stability along the pass is introduced next.

4.2 Stability along the pass for inferential ILC

The following definition for stability along the pass is adopted from [8, Definition 2.2.1, pp. 57].

Definition 7 *The dLRP in (7) is called stable along the pass if $\exists M_\infty > 0$ and $\gamma_\infty \in (0, 1)$, independent of α , such that*

$$\|\mathcal{Y}_k - \mathcal{Y}_\infty\| \leq M_\infty (\gamma_\infty)^k \Gamma_\infty(\mathcal{Y}_0, \mathcal{U}_\infty, \gamma_\infty), \quad \forall k \geq 0. \quad (11)$$

Here, Γ_∞ a constant that depends on the initial pass profile $\mathcal{Y}_0, \mathcal{U}_\infty, \gamma_\infty$, and matrices $\mathcal{A}, \mathcal{B}, \mathcal{C}$, and \mathcal{D} .

The essential difference with asymptotic stability is that constants M_∞ and γ_∞ are independent of α , and that (11) is also valid for the case $\alpha \rightarrow \infty$. An expression for Γ_∞ is given in [8, Definition 2.2.1, pp. 57]. A test for stability along the pass for inferential ILC system (7) is given next as an auxiliary result, which is used later on. The effect of Definition 7 is clarified directly after.

Lemma 8 (Stability along the pass) *Given the dLRP (7), where $\{\mathcal{A}, \mathcal{B}_0\}$ is controllable and $\{\mathcal{C}, \mathcal{A}\}$ is observable. Then, (7) is stable along the pass if and only if the following three conditions hold:*

- (1) $\rho(\mathcal{D}_0) < 1$,
- (2) $\rho(\mathcal{A}) < 1$,
- (3) $\rho(G(z)) < 1, \forall |z| = 1, z \in \mathbb{C}$,
with $G(z) = \mathcal{C}(zI - \mathcal{A})^{-1}\mathcal{B}_0 + \mathcal{D}_0$.

Proof See Appendix A.

Theorem 9 *If a dLRP is stable along the pass, then $\rho(\mathcal{A}_\infty) < 1$ in (9).*

Proof See Appendix A.

The proof of Lemma 8 in Appendix A reveals that if conditions 2 and 3 hold then condition 1 holds automatically: if the dLRP is stable along the pass then it is also asymptotically stable. Furthermore, Theorem 9 reveals that if a dLRP is stable along the pass, then $\rho(\mathcal{A}_\infty) < 1$. Hence, stability along the pass indeed leads to a stable limit profile. If algorithm (1) is stable along the pass then the stability issues that are present in Example 1 in Section 2.2 cannot occur.

Remark 1 *Several stability notions for dLRPs exist that also ensure $\rho(\mathcal{A}_\infty) < 1$, see e.g., [13,14]. The results in the present paper can directly be extended to this case.*

Conditions for stability long the pass of inferential ILC algorithm (1) are presented in the following theorem.

Theorem 10 *Given is dLRP (7) with matrices $\mathcal{A}, \mathcal{B}, \mathcal{B}_0, \mathcal{C}, \mathcal{D}$, and \mathcal{D}_0 in (8). Suppose that $\{\mathcal{A}, \mathcal{B}_0\}$ is controllable and $\{\mathcal{C}, \mathcal{A}\}$ is observable. Then, (7) is stable along the pass if and only if the following conditions hold*

- (1) $\rho(\bar{Q}(I - \bar{L}\bar{J})) < 1$,
- (2) (a) $\rho(A^{CP}) < 1$,
(b) $\rho(A^L) < 1$,
(c) $\rho(A^Q) < 1$,
- (3) $\rho(Q(z)(I - L(z)J(z))) < 1, \forall |z| = 1, z \in \mathbb{C}$.

with

$$J(z) = \frac{P^z(z)}{1 + C(z)P^y(z)}, \quad (12)$$

$\bar{Q}, \bar{L}, \bar{J}$ finite-time matrix representations of Q, L and J , and

$$A^{CP} = \begin{bmatrix} A^P & B^P C^C \\ -B^C C^P y & A^C - B^C D^P y C^C \end{bmatrix} \quad (13)$$

the system matrix of the closed-loop connection of C and P .

Proof (1) Follows from Theorem 4. (2) Note that $\lambda(\mathcal{A}) = \{\lambda(A^{CP}), \lambda(A^L), \lambda(A^Q)\}$. Hence, $\rho(\mathcal{A}) < 1 \Leftrightarrow \rho(A^{CP}) < 1, \rho(A^L) < 1, \rho(A^Q) < 1$. (3) Substituting $\mathcal{A}, \mathcal{B}_0, \mathcal{C}$ and \mathcal{D}_0 in (8) in condition 3 in Lemma 8 yields $G(z) = Q(z)(1 - L(z)J(z))$, and hence $\rho(G(z)) < 1 \Leftrightarrow \rho(Q(z)(1 - L(z)J(z))) < 1$.

Theorem 10 shows that stability along the pass has several connections to well-known convergence conditions in ILC. First, asymptotic stability of the dLRP corresponds to the finite-time convergence criterion in [4, Theorem 1]. Second, stability along the pass demands that the time domain dynamics for a fixed pass k are stable. In the inferential ILC setting, this demands L and Q filters that are strictly stable, and $\rho(A^{CP}) < 1$, i.e., C is an internally stabilizing controller. Third, Theorem 10 reveals that the third condition for stability along the pass is equivalent to the well-known frequency domain convergence criterion $\rho(Q(z)(1 - L(z)J(z))) < 1$, as is developed in, e.g., [4, Theorem 6].

In contrast, traditional ILC analysis and designs [3] involves weaker stability conditions than presented in Theorem 10. Typically, first an internally stabilizing feedback controller satisfying condition 2a in Theorem 10 is designed and then a (monotonically) convergent ILC algorithm, satisfying condition 1 and optionally 3. In this case there is no guarantee that $\rho(\mathcal{A}_\infty) < 1$. This is precisely the issue that arises in Example 1. Clearly, a stable limit profile is a key requirement.

A convergent ILC algorithm is assumed in Example 1 in Section 2.2. Next, it is shown that this result holds for any L if C includes integral action and $Q = 1$.

Theorem 11 *Given $Q = 1, P(z) = \begin{bmatrix} P^z(z) \\ P^y(z) \end{bmatrix}$, and C with minimal state-space representation A^C, B^C, C^C, D^C , satisfying $\rho(A^{CP}) < 1$ in (13) and $1 \in \lambda(A^C)$. Then, for any*

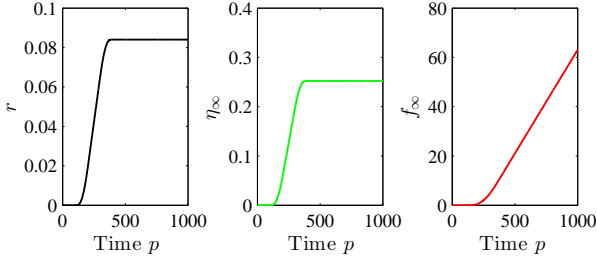


Fig. 5. Reference r (left), stable limit profile η_∞ for the serial structure (center), unstable limit profile f_∞ for the parallel structure (right).

The resulting closed-loop system $z_k = J_{ser}\eta_k$ is given by

$$z_k = \underbrace{\begin{bmatrix} A^{J_{ser}} & B^{J_{ser}} \\ C^{J_{ser}} & D^{J_{ser}} \end{bmatrix}}_{J_{ser}} \eta_k,$$

with $A^{J_{ser}} = 0.4$, $B^{J_{ser}} = 0.4$, $C^{J_{ser}} = 0.2$, and $D^{J_{ser}} = 0.2$. Clearly, the closed-loop system is asymptotically stable since $\rho(A^{J_{ser}}) < 1$. Let the learning filter $L = 5$, and robustness filter $Q = 1$. The three conditions for stability along the pass are verified next using Corollary 12.

The first condition $\rho(\bar{Q}(I - \bar{L}\bar{J}_{ser})) = 0$, since $1 - LD^{J_{ser}} = 0$, hence the underlying dLRP is asymptotically stable. The second condition only demands $\rho(A^{J_{ser}}) < 1$ since $A^L = \emptyset$ and $A^Q = \emptyset$. This is indeed the case as already shown. The third condition requires $\rho(Q(I - LJ_{ser}(z))) < 1, \forall |z| = 1, z \in \mathbb{C}$, and it can be verified that $Q(1 - LJ_{ser}(z)) = \begin{bmatrix} 0.4 & 0.4 \\ -1 & 0 \end{bmatrix}$.

Using the latter, the third condition is also satisfied since $\rho(Q(1 - LJ_{ser}(z))) \leq \frac{2}{3}, \forall |z| = 1, z \in \mathbb{C}$. Consequently, the resulting limit profile is asymptotically stable. This is verified next by using Corollary 12 and Theorem 6. The

limit profile is given by $\begin{bmatrix} \eta_\infty \\ e_\infty^z \end{bmatrix} = \begin{bmatrix} 0 & 2 \\ -1 & 5 \\ 0 & 0 \end{bmatrix} r$. Clearly, the limit

profile is asymptotically stable, and the resulting $e_\infty^z = 0$. Figure 5 shows an example reference r , the corresponding limit profile η_∞ , and the limit profile f_∞ from the parallel structure in (4). It is shown that the serial structure can eliminate the stability issues that are illustrated in Example 1. The results in Fig. 5 also show that in case the trial length is sufficiently short with respect to the growth rate in f_∞ , an ILC that is unstable along the pass could be relevant in practice since in this case the signal growth remains small and may not be a safety hazard.

6 Stability of classical $y = z$ ILC

In the traditional ILC case with $y = z$, see e.g., [3,15], the state-space system for f_∞ in (10) is non-minimal since $B^C(I - D^{Py}D^{Pz^{-1}}) = 0$ in (10) if $D^{Py} = D^{Pz}$. The states associated with A^C in (10) are not controllable. This

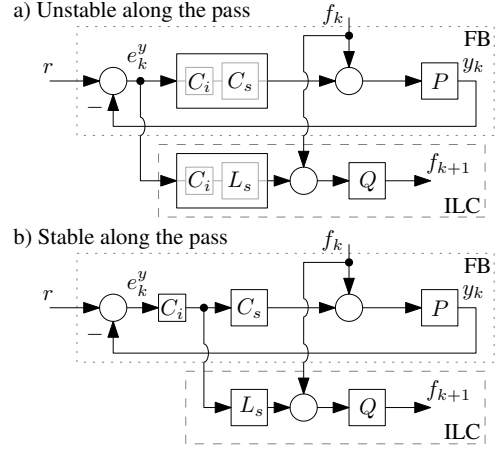


Fig. 6. Classical $y = z$ case, with C including integral action. a) The traditional implementation cannot be stable along the pass and may cause issues in practice. b) Solution with L_s

suggests that the input-output behavior of (10) is stable, even if $\rho(A^C) = 1$ when C includes integral action. The diagram in Fig. 6a shows the $y = z$ situation, where C and L contain C_i integrators. In practice, numerical integration errors in the states of the integrators may cause the control signals of the ILC and feedback controller to drift from trial to trial. The results in Theorem 11 are also valid for the traditional $y = z$ case, as is illustrated in the following corollary.

Corollary 13 Given $Q = 1$, a system $y = P(z)u$, and an internally stabilizing C with $1 \in \lambda(A^C)$. Then, for any learning filter L follows that either condition 2 or condition 3 for stability along the pass in Theorem 10 is violated.

Proof Follows from Theorem 11, with $P^y = P^z = P$.

The latter shows that if C includes integral action and $Q = 1$, also classical ILC implementations are not stable along the pass. Besides resorting to the serial ILC structure in Section 5, an alternative approach is presented in Fig. 6 and is related to a similar solution in optimal controller synthesis that relies on re-arranging the loop structure, see also [16] for related ideas. Suppose C and L include integral action. Let $C(z) = C_i(z)C_s(z)$, with C_i the integrators, and $C_s(z)$ strictly stable. Then apply ILC algorithm $f = Q(f + L_s C_i e_k^y)$. The key idea is to use $C_i e_k^y$ as an extra output of the controller, as shown in Fig. 6.

Stability along the pass directly follows by setting $J(z) := J_{stab}(z)$ in Theorem 10, with $J_{stab}(z) = \frac{C_i(z)P(z)}{1 + C_i(z)C_s(z)P(z)}$. Since $\lim_{z \rightarrow 1} J(z) = C_s^{-1}(z)$ with C_s strictly stable, the learning filter does not need to include integral action if C includes integral action and $\rho(A^L) < 1$. Hence, stability along the pass can be achieved with the proposed change in structure. This in turn guarantees a stable limit profile, leading to a stable ILC implementation.

7 Conclusion

Stability problems with inferential ILC are analyzed and solutions are proposed. It is shown that directly casting common control structures to the inferential setting can lead to configurations that are not stable in a 2D systems setting.

This aspect is analyzed by casting the time-trial dynamics into a discrete linear repetitive process, which is a class of 2D systems. To facilitate the analysis of the inferential control structure, the 2D stability notion of stability along the pass is translated to conditions on the ILC algorithm.

If the feedback controller includes integral action, the resulting ILC-feedback combination cannot be stable in a 2D sense. Solutions are presented and rely on changing the controller structure from a parallel to a serial configuration. In addition, insights in classical ILC where the performance variables are also used for feedback control are obtained.

Inferential ILC has important application areas such as printing systems, see [9]. Ongoing research is towards more experimental implementations and inter-sample behavior.

Acknowledgements

The authors would like to acknowledge fruitful discussions with and the contributions of Sjirk Koekebakker and Maarten Steinbuch. This work is supported by Océ Technologies, P.O. Box 101, 5900 MA Venlo, The Netherlands. This work is also supported by the Innovational Research Incentives Scheme under the VENI grant "Precision Motion: Beyond the Nanometer" (no. 13073) awarded by NWO (The Netherlands Organization for Scientific Research) and STW (Dutch Science Foundation).

Acknowledgements

The authors would like to acknowledge fruitful discussions with and the contributions of Sjirk Koekebakker and Maarten Steinbuch.

A Appendix auxiliary results

Definition 14 *The characteristic polynomial of (7) equals*

$$\varphi(z_1, z_2) := \det \begin{pmatrix} I - z_1 A & -z_1 B_0 \\ -z_2 C & I - z_2 D_0 \end{pmatrix}, z_1, z_2 \in \mathbb{C}. \quad (\text{A.1})$$

See [17] and [8, eq. (1.52), pp 36] for equivalent definitions.

Lemma 15 *Given a characteristic polynomial $\varphi(z_1, z_2)$ with $z_1, z_2 \in \mathbb{C}$, then $\varphi(z_1, z_2) \neq 0 \forall |z_1| \leq 1, \forall |z_2| \leq 1$ iff*

$$(1) \varphi(z_1, 0) \neq 0 \forall |z_1| \leq 1,$$

$$(2) \varphi(z_1, z_2) \neq 0 \forall |z_1| = 1, |z_2| \leq 1.$$

In the latter, the role of z_1 and z_2 may be interchanged.

Proof *These conditions are presented in [18].*

Proof Lemma 8 Given the controllability and the observability requirements, [8, Theorem 2.2.8, pp 64] reveals that the dLRP is stable along the pass if and only if

$$\varphi(z_1, z_2) \neq 0, \forall z_1, z_2 \in \mathbb{C}, |z_1| \leq 1, |z_2| \leq 1. \quad (\text{A.2})$$

Applying [19, Proposition 2.8.3] to (A.2) yields $\varphi(z_1, z_2) = \det(I - z_1 A) \det(I - z_2 G(z_1))$ with $G(z_1) = C(z_1 I - A)^{-1} B_0 + D_0$. Using Lemma 15 in Appendix A yields that condition (A.2) is equivalent to satisfying

$$(1) \det(z_1 I - A) \neq 0 \forall |z_1| \leq 1, \\ (2) \det(I - z_2 G(z_1)) \neq 0, \forall |z_1| = 1, |z_2| \leq 1.$$

These conditions are satisfied iff $\rho(A) < 1$ and $\rho(G(z_1)) < 1, \forall |z_1| = 1$, corresponding to conditions 2 and 3 in Lemma 8, respectively. Interchanging z_1 and z_2 in Lemma 15 yields that also $\rho(D_0) < 1$.

Proof Theorem 9 Applying [19, Proposition 2.8.4] to (A.1) yields characteristic polynomial $\varphi(z_1, z_2) = \det(I - z_2 D_0) \det(I - z_1 H(z_2))$, with $H(z_2) = B_0(I z_2 - D_0)^{-1} C + A$. Applying Lemma 15 yields $\rho(H(z_2)) < 1, \forall |z_2| = 1$. From (9) follows $\mathcal{A}_\infty = H(z_2 = 1)$, hence $\rho(\mathcal{A}_\infty) < 1$ if dLRP (7) is stable along the pass.

References

- [1] J. Parrish and C. Brosilow, "Inferential Control Applications," *Automatica*, vol. 21, no. 5, pp. 527–538, 1985.
- [2] T. Oomen, E. Grassens, and F. Hendriks, "Inferential Motion Control: Identification and Robust Control Framework for Positioning an Unmeasurable Point of Interest," *IEEE Trans. Contr. Syst. Techn.*, vol. 23, pp. 1602–1610, 2015.
- [3] D. Bristow, M. Tharayil, and A. Alleyne, "A Survey of Iterative Learning Control: a Learning-based Method for High-performance Tracking Control," *IEEE Contr. Syst. Mag.*, vol. 26, pp. 96–114, 2006.
- [4] M. Norrlöf and S. Gunnarsson, "Time and Frequency Domain Convergence Properties in Iterative Learning Control," *Int. J. Contr.*, vol. 75, pp. 1114–1126, 2002.
- [5] Y. Wang, F. Gao, and F. Doyle, "Survey on Iterative Learning Control, Repetitive Control, and Run-to-Run Control," *J. Proc. Cont.*, vol. 19, pp. 1589–1600, 2009.
- [6] R. Longman and C.-P. Lo, "Generalized Holds, Ripple Attenuation, and Tracking Additional Outputs in Learning Control," *J. Guid., Contr., Dyn.*, vol. 20, pp. 1207–1214, 1997.
- [7] J. Wallén, M. Norrlöf, and S. Gunnarsson, "A Framework for Analysis of Observer-based ILC," *Asian Journal of Control*, vol. 13, pp. 3–14, 2011.
- [8] E. Rogers, K. Galkowski, and D. Owens, *Control Systems Theory and Applications for Linear Repetitive Processes*. Springer-Verlag, 2007.

- [9] J. Bolder, T. Oomen, S. Koekebakker, and M. Steinbuch, "Using Iterative Learning Control with Basis Functions to Compensate Medium Deformation in a Wide-format Inkjet Printer," *Mechatronics*, vol. 24, pp. 944–953, 2014.
- [10] J. Bolder, T. Oomen, and M. Steinbuch, "On Inferential Iterative Learning Control: with example to a printing system," *Proc. Americ. Contr. Conf., Portland, OR, USA*, pp. 1827–1832, 2014.
- [11] J. Bolder, T. Oomen, and M. Steinbuch, "Aspects in Inferential Iterative Learning Control: a 2D Systems Analysis," *Proc. Conf. Dec. Contr., Los Angeles, CA, USA*, pp. 3584–3589, 2014.
- [12] J. Edwards and D. Owens, *Analysis and Control of Multipass Processes*. Research Studies Press, 1982.
- [13] W. Paszke, P. Dabkowski, E. Rogers, and K. Gałkowski, "New Results on Strong Practical Stability and Stabilization of Discrete Linear Repetitive Processes," *Syst. Contr. Lett.*, vol. 77, pp. 22–29, 2015.
- [14] P. Dabkowski, K. Gałkowski, E. Rogers, and A. Kummert, "Strong Practical Stability and Stabilization of Discrete Linear Repetitive Processes," *Multidimensional Systems and Signal Processing*, vol. 20, pp. 311–331, 2009.
- [15] T. Liu, X. Wang, and J. Chen, "Robust PID Based Indirect-type Iterative Learning Control for Batch Processes with Time-varying Uncertainties," *J. Proc. Cont.*, vol. 24, pp. 95–106, 2014.
- [16] J. Krause, "Comments on Grimble's Comments on Stein's Comments on Rolloff of H^∞ Optimal Controllers," *IEEE Trans. Automat. Contr.*, vol. 37, p. 702, 1992.
- [17] P. Agathoklis and S. Foda, "Characteristic Polynomial Assignment in 2-dimensional Discrete Systems," *Proc. IEE*, vol. 135, pp. 253–256, 1988.
- [18] D. Davis, "A Correct Proof of Huang's Theorem on Stability," *IEEE Transactions on Acoustics, Speech and Signal Processing*, vol. 11, pp. 425–426, 1976.
- [19] D. Bernstein, *Matrix Mathematics*. Princeton university press, 2009.